Research Square

Preprints are preliminary reports that have not undergone peer review.
They should not be considered conclusive, used to inform clinical practice,
or referenced by the media as validated information.

Three-dimensional fractal analysis of region-specific trabecular changes six months after Le Fort I osteotomy using cone-beam computed tomography

Hilal Algül[1]

halgul@ankara.edu.tr

Ankara University

Mahzun Yıldız[2]

Ankara University

Anıl Kamal[2]

Ankara University

Emre Karahan[3]

Ankara University

Mehmet Emre Yurttutan[2]

Ankara University

Ayşe Tuba Altuğ[1]

Ankara University

Research Article

Keywords: Cone-Beam Computed Tomography, Fractals, Orthognathic Surgery, Osteotomy, Le Fort, Bone Remodeling

Posted Date: October 14th, 2026

DOI: https://doi.org/10.21203/rs.3.rs-11183959/v1

License: This work is licensed under a Creative Commons Attribution 4.0 International License.
Read Full License

Additional Declarations: No competing interests reported.

Abstract

Postoperative trabecular changes along the Le Fort I osteotomy line remain poorly characterised. This retrospective study evaluated preoperative-to-six-month changes in the radiographic trabecular pattern at bilateral piriform and zygomaticomaxillary osteotomy sites and examined whether these changes differed by site, region, or side. Fifty patients who underwent one-piece Le Fort I osteotomy during bimaxillary surgery were included. Preoperative and six-month postoperative cone-beam computed tomography volumes were registered using the anterior cranial base, and anatomically corresponding freehand polygonal volumes of interest were delineated at four osteotomy sites. Fractal dimension was calculated by three-dimensional box-counting using standardised image-processing settings. Fractal dimension was significantly lower at six months at all sites, with Holm-adjusted p values of 0.012–0.034 and mean differences of − 0.188 to − 0.259. Change magnitude did not differ among sites (p = 0.934), between sides, or between regions (both Holm-adjusted p = 1.000). Interobserver reliability was excellent, and changes in volume of interest were not associated with changes in fractal dimension. Anatomically matched three-dimensional analysis demonstrated persistent differences in the radiographic trabecular pattern at six months. Fractal dimension may complement conventional imaging assessment but should not be interpreted as a direct indicator of bone healing.

1. Introduction

Le Fort I osteotomy is widely used to correct maxillary skeletal deformities and enables three-dimensional repositioning of the maxilla through advancement, setback, impaction, inferior repositioning and rotation. These movements aim to establish an appropriate occlusal relationship and improve facial aesthetics in patients with dentofacial deformities [1, 2]. Maintenance of the surgical outcome depends partly on the mechanical stability of the repositioned maxilla and the biological response at the osteotomy site. Quantitative characterisation of postoperative bone changes may therefore contribute to a better understanding of the structural remodelling occurring at the osteotomy site [3].

Previous studies have primarily used computed tomography (CT) to assess bone changes following Le Fort I osteotomy, focusing on the defect area between osteotomised segments and the continuity of bone across the osteotomy site. Ueki et al. (2011) used three-dimensional CT reconstructions to evaluate bone healing within the gaps between maxillary segments and in the pterygomaxillary region [4]. In a subsequent study, images acquired one week and one year postoperatively were reconstructed using a predefined CT density threshold, and changes in bone-defect area were quantified on the anterior and lateral maxillary walls [5]. More recently, bone formation within the osteotomy gap was assessed using changes in defect area and CT density values [6]. The six-month postoperative period therefore represents a clinically relevant stage for assessing osseous remodelling, because structural maturation at the osteotomy site may still be ongoing [5, 6]. Although these approaches provide valuable information on macroscopic defect closure and mineralisation, they depend on selected density thresholds and do not directly characterise trabecular organisation. Consequently, reductions in defect

area or increases in density may not fully represent changes in the radiographic trabecular pattern at the osteotomy site.

Trabecular bone has a complex and irregular architecture. Fractal analysis provides an image-derived measure of the geometric complexity of the radiographic trabecular pattern, expressed numerically as fractal dimension (FD) [7]. However, FD is an image-derived indicator of trabecular organisation rather than a direct measure of bone quality, mechanical competence or the extent of healing. Heo et al. (2002) reported that FD values decreased during the early postoperative period following mandibular orthognathic surgery and subsequently approached preoperative levels during follow-up [8]. Studies of bilateral sagittal split ramus osteotomy have similarly demonstrated the use of fractal analysis for monitoring temporal changes in the trabecular pattern at osteotomy sites [9, 10]. Nevertheless, the available evidence is predominantly based on mandibular assessments using two-dimensional radiographic images. More recently, Alpaydın et al. (2026) evaluated the midpalatal suture and adjacent alveolar trabecular bone using two-dimensional regions selected from cone-beam computed tomography (CBCT) sections and reported significantly lower FD values six months after surgically assisted rapid maxillary expansion [11].

The thin cortical bone of the maxilla, its proximity to anatomical spaces such as the maxillary sinus and nasal cavity, and regional variation in trabecular architecture complicate the standardised assessment of its bone structure. The lateral piriform and zygomaticomaxillary buttresses are particularly relevant because they correspond to common fixation sites following Le Fort I osteotomy [3]. Previous research has also demonstrated that maxillary FD values may vary according to anatomical region and side [12]. Nevertheless, to our knowledge, no study has directly evaluated region-specific trabecular changes along the Le Fort I osteotomy line using three-dimensional fractal analysis of anatomically matched preoperative and postoperative CBCT volumes.

Accordingly, the primary aim of this study was to assess preoperative-to-six-month postoperative changes in FD separately at the right and left piriform and zygomaticomaxillary regions following Le Fort I osteotomy. The secondary aim was to determine whether the magnitude of these changes differed among the four measurement sites, between the piriform and zygomaticomaxillary regions, or between the right and left sides. The null hypotheses were that FD values would not differ between the preoperative and six-month postoperative assessments at any of the four sites and that the magnitude of change would not differ among sites, between anatomical regions, or between sides.

2. Materials and Methods

2.1. Study design and ethical approval

This retrospective longitudinal observational study evaluated changes in the radiographic trabecular pattern at the osteotomy sites by comparing fractal dimension values derived from cone-beam computed tomography images obtained preoperatively and at the six-month postoperative follow-up

after Le Fort I osteotomy. The study protocol was approved by the Ankara University Faculty of Dentistry Ethics Committee for Non-Clinical Scientific Research (date: 20 July 2026; decision no. : 24/13) and was conducted in accordance with the Declaration of Helsinki. Written informed consent for the use and publication of anonymised clinical and radiographic data was obtained from all patients.

The CBCT images were retrieved from the archives of the Department of Dentomaxillofacial Radiology, Faculty of Dentistry, Ankara University, Türkiye. All scans had previously been acquired for routine diagnostic assessment, surgical planning or postoperative follow-up; therefore, no additional imaging was performed for research purposes. All clinical and imaging data were anonymised before analysis.

2.2. Study sample and eligibility criteria

The study sample was identified through a retrospective review of the clinical and radiographic records of patients who underwent Le Fort I osteotomy as part of bimaxillary orthognathic surgery at the Department of Oral and Maxillofacial Surgery, Faculty of Dentistry, Ankara University, between January 2022 and February 2026. Preoperative CBCT images were defined as the baseline time point (T0), whereas postoperative CBCT images obtained at the six-month follow-up were defined as T1.

Patients were eligible for inclusion if they had undergone a one-piece Le Fort I osteotomy; their T0 and T1 CBCT images had been acquired using the same CBCT unit and imaging protocol; and the bilateral piriform and zygomaticomaxillary regions could be reliably evaluated by fractal analysis. The exclusion criteria were segmental Le Fort I osteotomy; craniofacial syndrome or cleft lip and/or palate; systemic disease or medication use with the potential to affect bone metabolism; a history of maxillofacial trauma or surgery before the index procedure; bone grafting within the osteotomy gap, and postoperative infection or any complication requiring reoperation. Patients were also excluded if postoperative CBCT images were unavailable or if marked motion or metal artefacts prevented reliable VOI definition at the measurement sites.

Of the 82 patients assessed for eligibility, 32 were excluded. The patient selection process and reasons for exclusion are presented in Fig. 1. Consequently, 50 patients were included in the final study sample.

2.3. Surgical procedure

All operations were performed by the same surgeon using a standardised one-piece Le Fort I osteotomy extending from below the piriform aperture to the pterygoid plates. Following down-fracture and mobilisation of the maxilla, the planned maxillary movement was performed, and rigid internal fixation was achieved using L-shaped plates, each secured with four screws. No bone grafting was performed at the osteotomy sites.

2.4. Sample size and power analysis

Sample size was calculated a priori using G*Power software (version 3.1.9.7; Heinrich Heine University Düsseldorf, Düsseldorf, Germany), based on separate within-patient comparisons of T0 and T1 FD values

in each of the four anatomical regions. As the Holm adjustment could not be specified directly in G*Power, a conservative Bonferroni-adjusted significance level of α = 0.0125 was used to control the family-wise Type I error rate across the four regional comparisons. Assuming a two-sided paired-samples t-test, Cohen's $d_z = 0.50$, and 80% power, the minimum required sample size was 48 patients. The final sample of 50 patients therefore exceeded this requirement.

2.5. CBCT acquisition protocol

All T0 and T1 CBCT scans were acquired using a NewTom 7G unit (CEFLA s.c., Verona, Italy) at 120 kVp, 243.01 mAs, an exposure time of 5.8 s, a field of view of 290 mm in diameter × 300 mm in height, and an isotropic acquisition voxel size of 0.15 mm. Patients were scanned in the supine position using a standard head support. Use of the same unit and acquisition protocol at both time points was confirmed from the DICOM metadata.

2.6. Registration and superimposition of T0 and T1 images

The T0 and T1 DICOM volumes were imported into SYNAPSE 3D software (V4.2EU; FUJIFILM Corporation, Tokyo, Japan), with T0 designated as the reference volume. T1 was rigidly registered to T0 using the surgically unaffected anterior cranial base as the anatomical reference, in accordance with previously validated CBCT-based registration approaches [13–15]. Following registration, the volumes were superimposed, and alignment was visually verified in the axial, coronal and sagittal planes (Fig. 2).

The intersections of the osteotomy line with the bilateral piriform and zygomaticomaxillary regions were identified on T1. As no osteotomy line was present at T0, the centre of each T1 measurement site was transferred through the registered coordinate system to the corresponding preoperative bone location on T0. These matched locations were used as the centres for VOI placement at both time points. Registration was used solely for anatomical matching; FD measurements were performed on the untransformed T0 and T1 analysis datasets exported to CTAn using identical image-processing settings.

2.7. VOI definition and placement

Four measurement sites were defined for each patient: the right and left piriform and zygomaticomaxillary regions (Fig. 3). Each region was evaluated at T0 and T1, resulting in eight volumes of interest (VOIs) per patient and 400 VOIs overall. Owing to the anatomical characteristics of the maxilla, freehand polygonal VOIs adapted to the trabecular bone boundaries were used instead of fixed-shape geometric VOIs.

For each region, the axial T1 slice on which the osteotomy line was most clearly visualised was selected as the central slice. This slice, together with four consecutive superior and four consecutive inferior slices, formed a nine-slice VOI with a craniocaudal depth of approximately 2.70 mm at an isotropic analysis voxel size of 0.30003 mm. The corresponding central location and slice range at T0 were determined using the registered and superimposed volumes. Thus, VOI location and depth were anatomically matched between T0 and T1, whereas the contours were delineated separately according to the trabecular bone boundaries at each time point.

The piriform and zygomaticomaxillary VOIs were delineated within the medullary bone at the intersections of the osteotomy line with the lateral piriform and zygomaticomaxillary buttresses, respectively. Polygonal contours were manually drawn on the central, most superior and most inferior slices. Intermediate contours were generated by interpolation in CTAn and manually corrected when necessary. The VOIs included trabecular bone while excluding the nasal cavity, maxillary sinus, cortical bone, tooth roots, periodontal ligament space and fixation hardware. Identical criteria were applied to both sides and time points, and VOI placement was not modified according to the resulting FD value.

2.8. Three-dimensional fractal analysis

The polygonal VOIs were analysed using CTAn software (version 1.18.4.0+; Bruker microCT, Kontich, Belgium). Before analysis, all datasets were uniformly resampled to a fixed isotropic voxel size of 0.30003 mm. Images were processed as 8-bit greyscale data without additional filtering or morphological processing and were binarised using a predefined fixed threshold range of 80–110 on the 8-bit scale. Identical thresholding and analysis settings were applied to all measurements. Fractal dimension (FD) was calculated using the Kolmogorov box-counting algorithm implemented in the 3D Analysis module of CTAn. The image-processing workflow is illustrated in Fig. 4. The physical volume of each VOI was automatically calculated in mm^3 and recorded to assess the temporal consistency of VOI size at each measurement site.

2.9. Interobserver measurement reliability

All T0 and T1 measurements from 16 randomly selected patients were independently repeated by a second observer who was blinded to the first observer's results. The repeat assessment covered the entire measurement workflow, including image registration, measurement-site identification, VOI delineation, volume recording and FD calculation. Interobserver reliability for fractal dimension values and volumes of interest was assessed using two-way random-effects, single-measure, absolute-agreement intraclass correlation coefficients, with 95% confidence intervals, separately for each combination of time point, anatomical region, and side. ICC values greater than 0.90 were interpreted as indicating excellent reliability.

2.10. Statistical analyses

Statistical analyses were performed using IBM SPSS Statistics for Windows, version 26.0 (IBM Corp., Armonk, NY, USA). Distributional assumptions for change scores were evaluated using skewness and kurtosis, with values between − 2 and + 2 considered acceptable. Continuous variables were summarised as mean ± standard deviation or mean with 95% confidence intervals, as appropriate. Mean differences were reported with 95% confidence intervals, and categorical variables were presented as frequencies and percentages.

The primary outcome was the site-specific change in FD from T0 to T1. Paired-samples *t*-tests were performed separately for the right and left piriform and zygomaticomaxillary regions, with Holm adjustment applied across the four primary comparisons. Change scores were calculated as ΔFD = T1 −

T0, and differences among the four site-specific change scores were assessed using one-way repeated-measures analysis of variance. For the planned secondary comparisons, side-specific changes were calculated by averaging the piriform and zygomaticomaxillary ΔFD values on each side, whereas region-specific changes were calculated by averaging the right and left ΔFD values within each anatomical region. Right–left and piriform–zygomaticomaxillary changes were compared using paired-samples *t*-tests, with Holm adjustment applied across these two comparisons. VOI volumes were compared between T0 and T1 separately at each of the four measurement sites using paired-samples *t*-tests, with Holm adjustment applied across the four comparisons. As an exploratory sensitivity analysis, Pearson correlation coefficients were calculated separately for each site to examine the association between changes in VOI volume (ΔVOI = T1 − T0) and changes in FD (ΔFD = T1 − T0), with Holm adjustment applied across the four correlations. Effect sizes were expressed as Cohen's d_z for paired-samples *t*-tests and partial eta squared (η_p^2) for repeated-measures analyses. A two-sided $p < 0.05$ was considered statistically significant; Holm-adjusted *p* values were used for each predefined family of multiple comparisons.

3. Results

3.1. Patient selection and characteristics

Of the 82 patients assessed for eligibility, 50 met the inclusion criteria and were included in the final analysis (Fig. 1). Complete measurements were available for all four anatomical sites at both time points, resulting in 400 VOIs. Patient demographic and clinical characteristics are summarised in Table 1.

Table 1
Demographic characteristics of the study sample (n = 50)

Characteristic	Value
Sex	**n (%)**
Female	33 (66.0)
Male	17 (34.0)
Age, years	
Mean ± SD	26.84 ± 4.37
Range	20.33–36.92

SD, standard deviation.

3.2. Interobserver reliability

Interobserver reliability was excellent, with ICC values ranging from 0.904 to 0.987 for FD measurements and from 0.914 to 0.969 for VOI volume measurements.

3.3. Region-specific changes in fractal dimension

FD values were significantly lower at T1 than at T0 in all four measurement sites, with all differences remaining significant after Holm adjustment (adjusted $p = 0.012–0.034$; Table 2).

Table 2
Region-specific changes in fractal dimension from T0 to T1 (n = 50)

Region	T0, mean ± SD	T1, mean ± SD	ΔFD, mean (95% CI)	*t*	Holm-adjusted *p*	Cohen's d_z
Right piriform	1.623 ± 0.493	1.386 ± 0.362	−0.236 (−0.399 to −0.074)	−2.918	0.016	−0.413
Right zygomaticomaxillary	1.676 ± 0.431	1.465 ± 0.546	−0.211 (−0.405 to −0.016)	−2.176	0.034	−0.308
Left piriform	1.619 ± 0.422	1.431 ± 0.364	−0.188 (−0.340 to −0.036)	−2.491	0.032	−0.352
Left zygomaticomaxillary	1.679 ± 0.486	1.420 ± 0.431	−0.259 (−0.426 to −0.092)	−3.111	0.012	−0.440

Data were analysed using paired-samples t-tests. ΔFD was calculated as T1 − T0; therefore, negative values indicate lower FD at T1. The p values were adjusted across the four comparisons using the Holm method. FD, fractal dimension; T0, preoperative assessment; T1, six-month postoperative assessment; SD, standard deviation; CI, confidence interval; d_z, paired-samples Cohen's d.

3.4. Regional and side-related comparisons of FD changes

The magnitude of FD change did not differ significantly among the four measurement sites ($p = 0.934$; Table 3). Similarly, no significant differences in FD change were observed between the right and left sides or between the piriform and zygomaticomaxillary regions (both Holm-adjusted $p = 1.000$; Table 4).

Table 3
Comparison of FD changes among the four measurement sites (n = 50)

Region	ΔFD, mean ± SD	95% CI	F(3, 147)	*p*	ηp^2
Right piriform	−0.236 ± 0.572	−0.399 to − 0.074			
Right zygomaticomaxillary	−0.211 ± 0.686	−0.405 to − 0.016			
Left piriform	−0.188 ± 0.534	−0.340 to − 0.036			
Left zygomaticomaxillary	−0.259 ± 0.589	−0.426 to − 0.092			
Overall comparison			0.143	0.934	0.003

ΔFD was calculated as T1 − T0. Differences among the four measurement sites were analysed using one-way repeated-measures analysis of variance. FD, fractal dimension; SD, standard deviation; CI, confidence interval; η_p^2, partial eta squared.

Table 4
Comparisons of FD changes according to side and anatomical region (n = 50)

Comparison	Mean ΔFD	Contrast	95% CI of contrast	*p*	Holm-adjusted *p*	Cohen's d_z
Side	−0.223	Left − right: −0.0001	−0.158 to 0.158	0.999	1.000	< 0.001
Right	− 0.224					
Left						
Anatomical region	−0.212	Zygomaticomaxillary − piriform: −0.022	−0.181 to 0.137	0.779	1.000	−0.040
Piriform	−0.235					
Zygomaticomaxillary						

ΔFD was calculated as T1 − T0. For the side comparison, ΔFD values were averaged across the piriform and zygomaticomaxillary regions; for the anatomical-region comparison, they were averaged across the right and left sides. Contrasts were calculated as left − right and zygomaticomaxillary − piriform. Comparisons were performed using paired-samples t-tests, and p values were adjusted across the two comparisons using the Holm method. FD, fractal dimension; T0, preoperative assessment; T1, six-month postoperative assessment; CI, confidence interval; d_z, paired-samples Cohen's d.

3.5. VOI volume assessment

After Holm adjustment, VOI volumes did not differ significantly between T0 and T1 in the right piriform, right zygomaticomaxillary, or left piriform regions. A small but statistically significant reduction was observed in the left zygomaticomaxillary region (mean T1 − T0 difference, − 0.022 mm^3; 95% CI, − 0.034

to − 0.010; Holm-adjusted $p = 0.003$; Table 5). Changes in VOI volume were not significantly correlated with changes in FD at any region (correlation coefficients, − 0.119 to 0.158; all Holm-adjusted $p = 1.000$).

Table 5
Site-specific comparison of VOI volumes between T0 and T1 (n = 50)

Measurement site	T0, mean ± SD (mm^3)	T1, mean ± SD (mm^3)	ΔVOI, mean (95% CI) (mm^3)	*t*	Holm-adjusted *p*	Cohen's d_z
Right piriform	13.183 ± 0.418	13.195 ± 0.427	0.012 (− 0.017 to 0.040)	0.829	1.000	0.117
Right zygomaticomaxillary	11.453 ± 0.403	11.457 ± 0.391	0.004 (− 0.013 to 0.021)	0.483	1.000	0.068
Left piriform	13.235 ± 0.405	13.235 ± 0.381	−0.0004 (− 0.019 to 0.018)	−0.043	1.000	−0.006
Left zygomaticomaxillary	11.485 ± 0.384	11.463 ± 0.377	−0.022 (− 0.034 to − 0.010)	−3.586	0.003	−0.507

VOI volumes are presented as mean ± standard deviation. ΔVOI was calculated as T1 − T0. Comparisons were performed using paired-samples t-tests, and p values were adjusted across the four comparisons using the Holm method. VOI, volume of interest; T0, preoperative assessment; T1, six-month postoperative assessment; CI, confidence interval; d_z paired-samples Cohen's d.

4. Discussion

This study assessed whether fractal dimension (FD) values in the bilateral piriform and zygomaticomaxillary osteotomy regions had returned to their preoperative levels six months after Le Fort I osteotomy. The principal finding was that FD values at six months remained significantly lower than their corresponding preoperative values in all four measurement sites, with mean T1 − T0 differences ranging from − 0.188 to − 0.259. However, the magnitude of FD change did not differ significantly among the four measurement sites, between the right and left sides, or between the piriform and zygomaticomaxillary regions. Taken together, these findings indicate that the radiographic trabecular structure at the osteotomy sites remained different from its preoperative state at six months by six months and that the observed change was broadly similar across the maxillary regions evaluated.

The CT-based studies by Ueki and colleagues (2011) provide the most anatomically and clinically relevant comparisons for the present findings [4]. Ueki et al. (2011) reported that bone defects in the anterior and lateral maxillary walls decreased in size within one year after Le Fort I osteotomy, although complete bone continuity was not achieved at every osteotomy site, particularly in the pterygomaxillary region [4]. Subsequent studies by the same group showed that defects in the anterior and lateral

maxillary walls did not consistently decrease within one year and that residual defects could persist in some regions [5, 6]. Local CT values were also reported to vary according to defect status and anatomical region [6]. Collectively, these observations suggest that radiographic bone changes following Le Fort I osteotomy may not occur at the same rate throughout the maxilla and may remain detectable beyond six months. Accordingly, the lower FD values observed in the present study at six months are broadly consistent with previous CT-based evidence that structural changes at maxillary osteotomy sites may persist beyond this interval.

Nevertheless, the CT-based outcomes evaluated by Ueki and colleagues—including macroscopic defect area, cortical continuity and local CT values—do not represent the same structural characteristics as the FD measurements used in the present study [6]. A reduction in the osteotomy defect or the establishment of cortical continuity does not necessarily indicate that the trabecular pattern has returned to its preoperative state. These approaches should therefore be regarded as complementary rather than equivalent radiographic assessments of different aspects of bone changes following Le Fort I osteotomy.

Previous studies evaluating temporal changes in FD at osteotomy sites following orthognathic surgery have predominantly focused on the mandible and used two-dimensional radiographic images. Heo et al. (2002) reported that FD values decreased at mandibular osteotomy sites during the early postoperative period and subsequently increased towards preoperative levels [8]. Following BSSRO, Çolak et al. (2023) found that FD values at the horizontal osteotomy line were no longer significantly different from preoperative values at six months, whereas values at the vertical osteotomy line remained significantly different until the 12-month assessment [9]. The authors attributed this regional difference to osteotomy geometry and the larger area of bone contact along the horizontal osteotomy line. Müftüoğlu and Karasu (2024) similarly observed an early postoperative reduction followed by an increase in FD, with values no longer differing significantly from their preoperative levels at 12 months [10].

Evidence from the maxilla remains limited and is not entirely consistent. Pergel et al. (2025) found no significant difference between preoperative and six-month FD values at the midline osteotomy region following surgically assisted rapid maxillary expansion [16]. More recently, Alpaydın et al. (2026) reported significantly lower FD values at six months in both the midpalatal suture and the adjacent alveolar trabecular bone following SARME [11]. The latter finding is consistent with the direction of change observed in the present study. However, Pergel et al. (2025) used a two-dimensional region on panoramic radiographs [16], whereas Alpaydın et al. analysed two-dimensional regions selected from CBCT sections [11]. In contrast, the present study evaluated anatomically matched three-dimensional VOIs positioned directly along the bilateral piriform and zygomaticomaxillary components of the Le Fort I osteotomy line. These differences indicate that postoperative FD findings may be influenced not only by the surgical procedure and anatomical site, but also by the imaging modality, ROI or VOI geometry and image-processing workflow.

The surgical and biomechanical differences among these procedures should also be considered. Surgically assisted rapid maxillary expansion involves localised bone separation followed by gradual transverse displacement, whereas Le Fort I osteotomy requires complete mobilisation and repositioning of the maxilla along a more extensive osteotomy line. BSSRO, in turn, may provide broad cancellous contact or overlap between the mandibular segments. These differences could influence the temporal pattern of trabecular reorganisation; however, because the procedures have not been compared directly using a standardised FD protocol, they cannot be considered established explanations for the differences among studies. Furthermore, absolute FD values should not be compared directly across studies employing different imaging and image-processing protocols.

Eriş et al. (2026) used three-dimensional CBCT-based fractal analysis to evaluate the mandibular condyle in patients undergoing bimaxillary orthognathic surgery and found no significant change in FD from the preoperative assessment to one year postoperatively, nor any difference between fixation types [17]. This study demonstrates the feasibility of applying CBCT-based three-dimensional FD analysis to the assessment of trabecular changes following orthognathic surgery. However, Eriş et al. (2026) evaluated the mandibular condyle, which is indirectly affected by surgery, at one year, whereas the present study directly examined maxillary sites along the Le Fort I osteotomy line at six months [17]. The differing findings should therefore be interpreted in light of differences in anatomical site, the nature of surgical involvement and follow-up duration.

FD is an image-derived quantitative measure of the geometric organisation of the trabecular pattern [7, 18, 19]. However, it does not directly measure bone mineral density, mechanical strength or histological healing. Accordingly, the lower FD values observed at six months indicate that the radiographic trabecular pattern at the osteotomy sites remained different from its preoperative state, but do not in themselves constitute evidence of delayed or incomplete bone healing. Although this difference may be associated with postoperative remodelling, the underlying biological process cannot be determined from FD measurements alone. FD may therefore complement conventional radiographic assessment of trabecular changes at Le Fort I osteotomy sites; however, the present findings do not establish an FD threshold for clinical decision-making.

The magnitude of FD change did not differ significantly among the four measurement sites, between the right and left sides, or between the piriform and zygomaticomaxillary regions, suggesting a no statistically detectable differences in the magnitude of change across the evaluated osteotomy sites. Although side-related differences in maxillary FD have previously been reported [12], the present analysis focused on differences in postoperative change rather than on absolute right–left FD values. The absence of a significant difference should therefore not be interpreted as evidence of biological equivalence, but only as the absence of a statistically detectable difference within the present sample and analytical framework.

A principal strength of this study was the region-specific assessment of trabecular changes along the Le Fort I osteotomy line at the piriform and zygomaticomaxillary regions. Given the anatomical

heterogeneity of the maxilla, analysing T1 – T0 changes separately at each site avoided obscuring local changes by combining all measurements into a single patient-level mean. Registration of the T0 and T1 volumes using the surgically unaffected anterior cranial base, followed by matching of the osteotomy sites identified at T1 with the corresponding regions at T0, enabled within-patient comparisons of anatomically corresponding sites. Methodological consistency was further supported by the use of the same CBCT unit and acquisition protocol and by the application of identical voxel size and image-processing settings to all datasets. The excellent interobserver reliability observed for both FD and VOI volume measurements further supported the reproducibility of the measurement workflow.

This study has several limitations. Its retrospective design and the availability of assessments only at the preoperative stage and six months postoperatively precluded evaluation of the early course of FD change and determination of whether preoperative levels would be reached over a longer follow-up period. However, obtaining early or repeated postoperative CBCT scans solely for research purposes, in the absence of a clinical indication, would not have been ethically justified because of the associated exposure to ionising radiation. The analyses were therefore restricted to images acquired as part of routine clinical follow-up.

The use of freehand polygonal VOIs adapted to the trabecular bone boundaries, rather than fixed geometric volumes, was another limitation necessitated by the complex anatomy of the maxilla. No statistically significant T0–T1 differences in VOI volume were detected at three measurement sites, whereas a small but statistically significant reduction was observed in the left zygomaticomaxillary region. Changes in VOI volume were not significantly associated with changes in FD at any site, reducing the likelihood that the primary findings were explained solely by variations in VOI size. Nevertheless, this analysis cannot completely eliminate variability arising from freehand VOI delineation, because VOIs of similar volume may differ in shape, boundaries and trabecular content. Indeed, Algül et al. showed that freehand and fixed geometric ROIs may produce findings in the same direction while yielding different absolute FD values [12]. The potential influence of VOI selection on FD measurements should therefore be acknowledged.

Finally, CBCT grey values may be influenced by the imaging unit, acquisition parameters, reconstruction procedure and thresholding method. Although all scans were obtained using the same CBCT unit and acquisition protocol and identical image-processing settings were applied, CBCT grey values are not standardised measures of tissue attenuation. Moreover, the analysis datasets were uniformly resampled from an acquisition voxel size of 0.15 mm to an isotropic voxel size of 0.30003 mm. Although this standardised the spatial resolution across all measurements, a potential influence of resampling on the calculated FD values cannot be excluded. The segmentation threshold was not validated against a histological or micro-CT reference, which limits the interpretation and external comparability of the absolute FD values. The absence of histological, mechanical or advanced microstructural validation further restricts the biological interpretation of the findings. The magnitude and direction of maxillary movement were not incorporated into the analysis; therefore, their potential influence on regional trabecular changes could not be determined. In addition, the single-centre design and exclusive inclusion

of patients undergoing bimaxillary orthognathic surgery may limit the generalisability of the results to patients treated with isolated Le Fort I osteotomy or different surgical protocols. Future multicentre studies using clinically indicated imaging records, longer follow-up periods and complementary structural measurements may provide a more comprehensive assessment of time-dependent trabecular changes at osteotomy sites.

At approximately six months after Le Fort I osteotomy, FD values in the bilateral piriform and zygomaticomaxillary osteotomy regions remained significantly lower than their respective preoperative values. No statistically significant differences in the magnitude of FD change were detected among the four measurement sites, between the piriform and zygomaticomaxillary regions, or between the right and left sides. These findings indicate that the radiographic trabecular pattern at the evaluated osteotomy sites remained different from its preoperative state at approximately six months. FD should therefore be regarded as a complementary imaging parameter for evaluating trabecular changes rather than as a direct indicator of biological or mechanical bone healing.

Declarations

Funding

This research received no specific grant from any funding agency in the public, commercial, or not-for-profit sectors.

Competing interest

The authors declare that they have no known competing financial interests or personal relationships that could have appeared to influence the work reported in this paper.

Ethics approval

The study protocol was approved by the Ankara University Faculty of Dentistry Ethics Committee for Non-Clinical Scientific Research (20 July 2026; decision no. 24/13) and was conducted in accordance with the Declaration of Helsinki.

Informed consent

Written informed consent for the use and publication of anonymised clinical and radiographic data was obtained from all patients.

Data availability

The datasets generated and analysed during the current study are not publicly available because they contain clinical imaging data but are available from the corresponding author on reasonable request, subject to institutional and ethical requirements.

References

1. Eshghpour M, Mianbandi V, Samieirad S. Intra- and postoperative complications of Le Fort I maxillary osteotomy. J Craniofac Surg. 2018;29:e797–803. https://doi.org/10.1097/SCS.0000000000004828.
2. Weiss RO 2nd, Ong AA, Reddy LV, Bahmanyar S, Vincent AG, Ducic Y. Orthognathic surgery—LeFort I osteotomy. Facial Plast Surg. 2021;37:703–8. https://doi.org/10.1055/s-0041-1735308.
3. Grillo R, Reis BAQ, Lima BC, Pinto LAPF, Melhem-Elias F. Comparison between 2- and 4-plate fixation in Le Fort I osteotomy: a mixed methods systematic review. Oral Surg Oral Med Oral Pathol Oral Radiol. 2025;139:289–98. https://doi.org/10.1016/j.oooo.2024.09.002.
4. Ueki K, Miyazaki M, Okabe K, Mukozawa A, Marukawa K, Moroi A, Nakagawa K, Yamamoto E. Assessment of bone healing after Le Fort I osteotomy with 3-dimensional computed tomography. J Craniomaxillofac Surg. 2011;39:237–43. https://doi.org/10.1016/j.jcms.2010.06.008.
5. Ueki K, Yoshizawa K, Moroi A. Bone healing after Le Fort I osteotomy with sagittal split ramus osteotomy using uHA/PLLA plates and screws in class II and III patients. J Craniomaxillofac Surg. 2019;47:1338–42. https://doi.org/10.1016/j.jcms.2019.06.006.
6. Ueki K, Gomi K, Takekawa T, Ono S, Takayama A, Yoshizawa K, Moroi A. Maxillary bone healing and CT value after Le Fort I osteotomy using an absorbable plate system: a retrospective study. J Craniomaxillofac Surg. 2024;52:727–32. https://doi.org/10.1016/j.jcms.2024.03.024.
7. Kato CNAO, Barra SG, Tavares NPK, Amaral TMP, Brasileiro CB, Mesquita RA, Abreu LG. Use of fractal analysis in dental images: a systematic review. Dentomaxillofac Radiol. 2020;49:20180457. https://doi.org/10.1259/dmfr.20180457.
8. Heo MS, Park KS, Lee SS, Choi SC, Koak JY, Heo SJ, Han CH, Kim JD. Fractal analysis of mandibular bony healing after orthognathic surgery. Oral Surg Oral Med Oral Pathol Oral Radiol Endod. 2002;94:763–7. https://doi.org/10.1067/moe.2002.128972.
9. Çolak S, Altan A, Bayrak S, Akbulut N. Evaluation of bony changes observed in mandibular osteotomy lines and mandibular condyles following bilateral sagittal ramus osteotomy by fractal analysis. Oral Maxillofac Surg. 2023;27:519–26. https://doi.org/10.1007/s10006-022-01101-x.
10. Muftuoglu O, Karasu HA. Assessment of mandibular bony healing, mandibular condyle and angulus after orthognathic surgery using the fractal dimension method. Med Oral Patol Oral Cir Bucal. 2024;29:e620–5. https://doi.org/10.4317/medoral.26587.
11. Derin Alpaydın F, Sunal Aktürk E, Kurt G, Dolanmaz D, Pergel T. Effects of surgically assisted rapid maxillary expansion on the anterior maxillary teeth and trabecular bone structure: a controlled clinical study. Clin Oral Investig. 2026;30:432. https://doi.org/10.1007/s00784-026-07096-z.
12. Algül H, Haksayar G, Toygar Memikoglu TU, Altug AT. Assessment of right–left differences in trabecular bone structure within the maxillary lateral incisor–canine region using fractal analysis. BMC Oral Health. 2026;26:1674. https://doi.org/10.1186/s12903-026-09728-y.

13. Almukhtar A, Ju X, Khambay B, McDonald J, Ayoub A. Comparison of the accuracy of voxel-based registration and surface-based registration for 3D assessment of surgical change following orthognathic surgery. PLoS ONE. 2014;9:e93402. https://doi.org/10.1371/journal.pone.0093402.
14. Cevidanes LHS, Bailey LJ, Tucker GR Jr, Styner MA, Mol A, Phillips CL, Proffit WR, Turvey TA. Superimposition of 3D cone-beam CT models of orthognathic surgery patients. Dentomaxillofac Radiol. 2005;34:369–75. https://doi.org/10.1259/dmfr/17102411.
15. da Costa Senior O, Vaes L, Mulier D, Jacobs R, Politis C, Shaheen E. Three dimensional assessment of segmented Le Fort I osteotomy planning and follow-up: a validation study. J Dent. 2021;111:103707. https://doi.org/10.1016/j.jdent.2021.103707.
16. Pergel T, Akkoyun EF, Alagoz EA. Assessment of bone density between central incisors using fractal analysis in patients undergoing surgically assisted rapid maxillary expansion. Niger J Clin Pract. 2025;28:595–601. https://doi.org/10.4103/njcp.njcp_892_24.
17. Eriş MA, Durmaz M, Haksayar G, Yurttutan ME, Kadıoğlu MB, Yıldız M, Kocamaz ÖF, Kolsuz ME. Three-dimensional fractal analysis of the mandibular condyle after bilateral sagittal split ramus osteotomy in class III patients: rigid versus semirigid fixation. Cranio. 2026. https://doi.org/10.1080/08869634.2026.2677042.
18. Geraets WG, van der Stelt PF. Fractal properties of bone. Dentomaxillofac Radiol. 2000;29:144–53. https://doi.org/10.1038/sj/dmfr/4600524.
19. Lopes R, Betrouni N. Fractal and multifractal analysis: a review. Med Image Anal. 2009;13:634–49. https://doi.org/10.1016/j.media.2009.05.003.

Figures

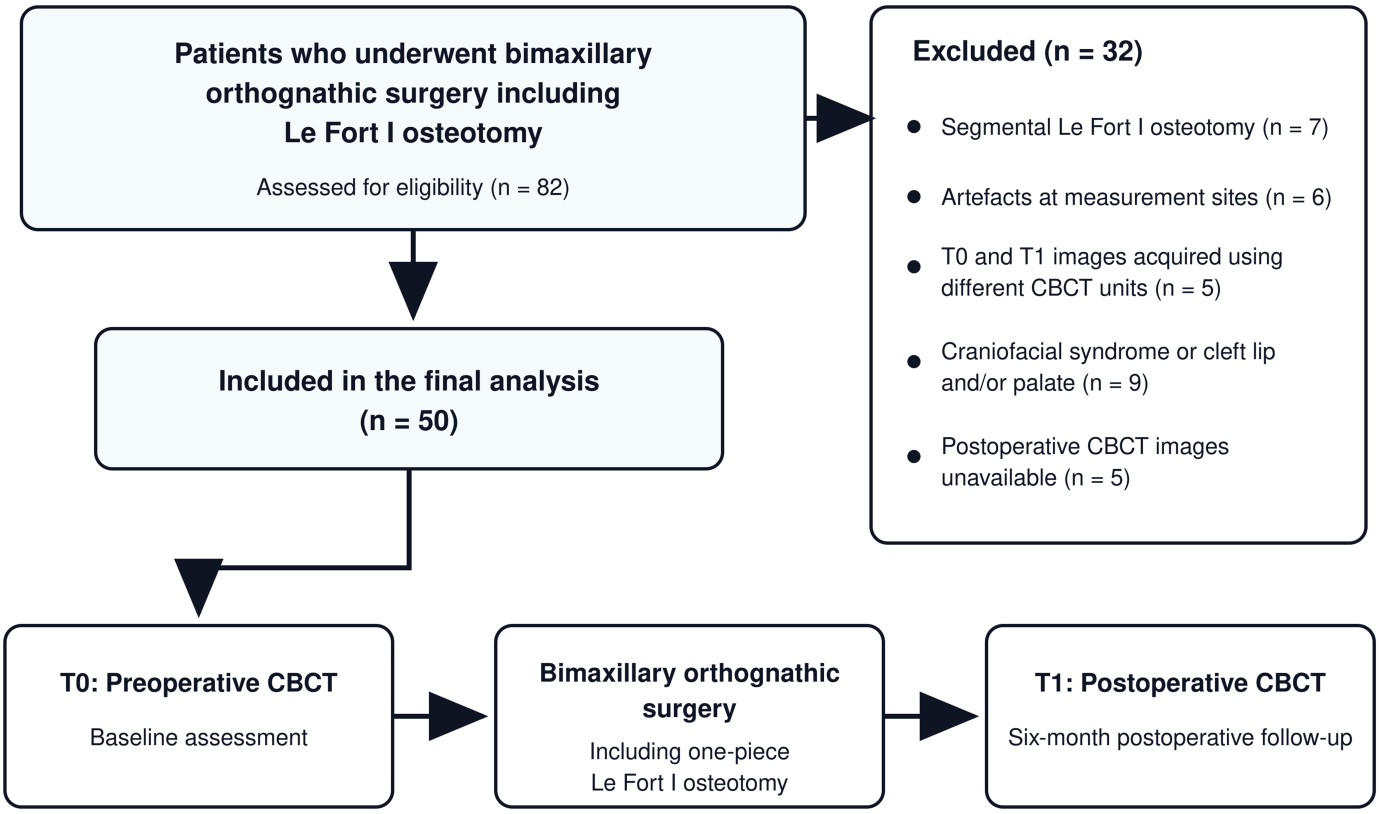


Figure 1

Flow diagram of patient selection and study time points. CBCT, cone-beam computed tomography; T0, preoperative assessment; T1, six-month postoperative assessment

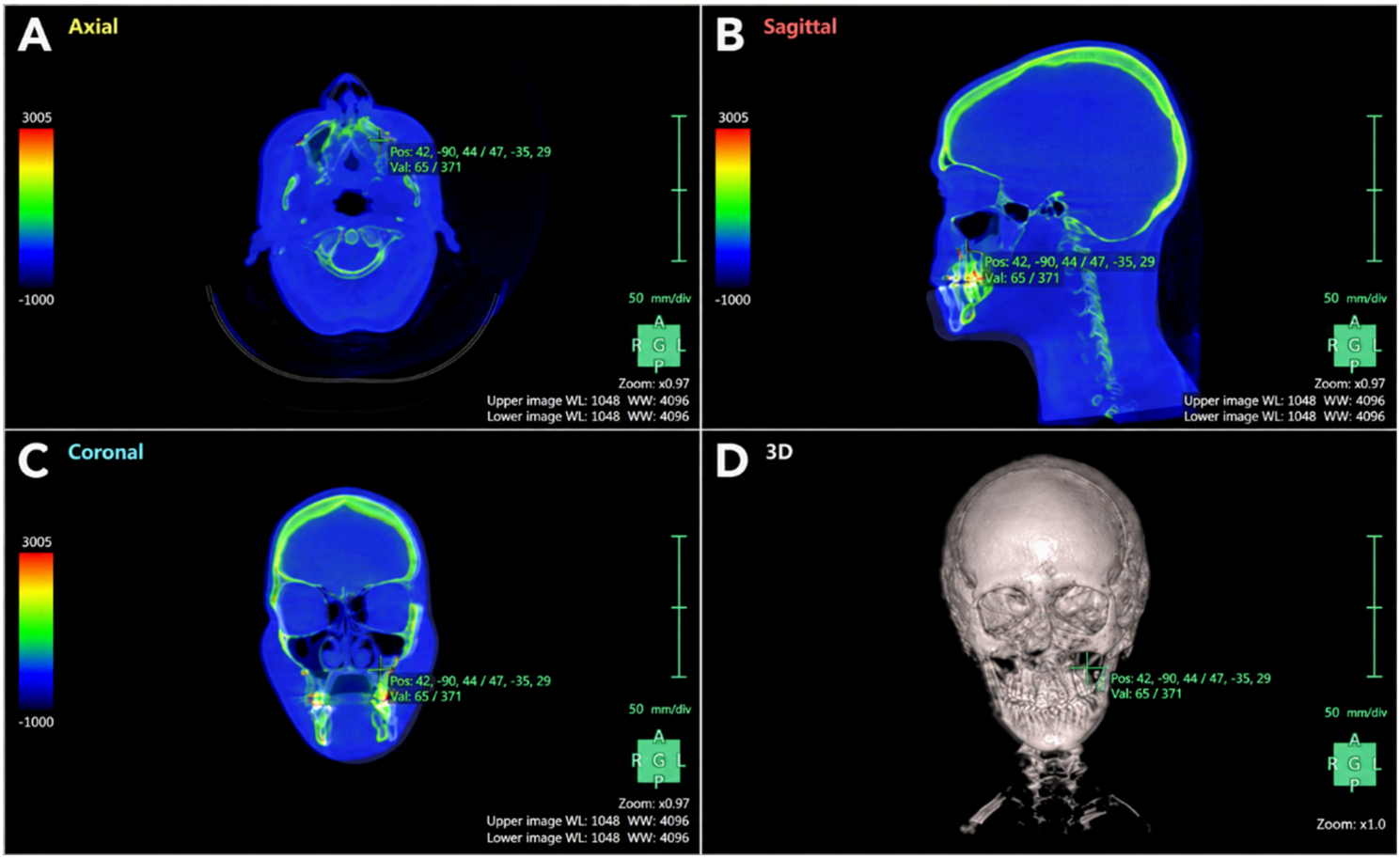


Figure 2

Rigid registration and superimposition of the preoperative (T0) and six-month postoperative (T1) CBCT volumes using the surgically unaffected anterior cranial base as the reference region. Registration was visually verified in the axial (A), sagittal (B) and coronal (C) planes and on the three-dimensional reconstruction (D). The T1 volume is displayed in colour, whereas the T0 volume is shown as a semi-transparent overlay. CBCT, cone-beam computed tomography

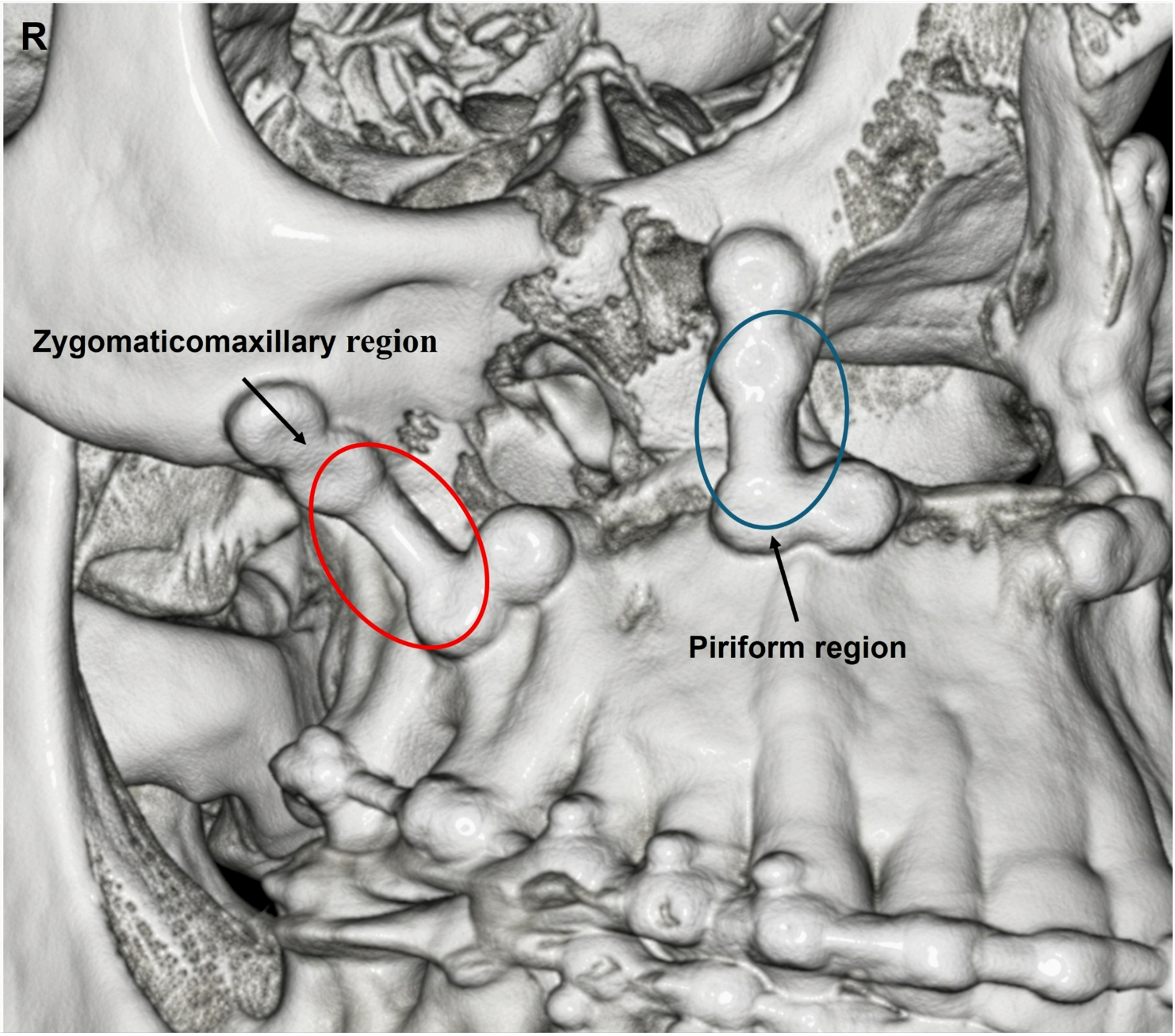


Figure 3

Three-dimensional reconstruction of a postoperative CBCT volume showing the anatomical localisation of the right piriform and zygomaticomaxillary measurement regions along the Le Fort I osteotomy line. The blue and red outlines indicate the piriform and zygomaticomaxillary regions, respectively, and represent anatomical localisation rather than the exact boundaries of the analysed VOIs. R, right side; VOI, volume of interest

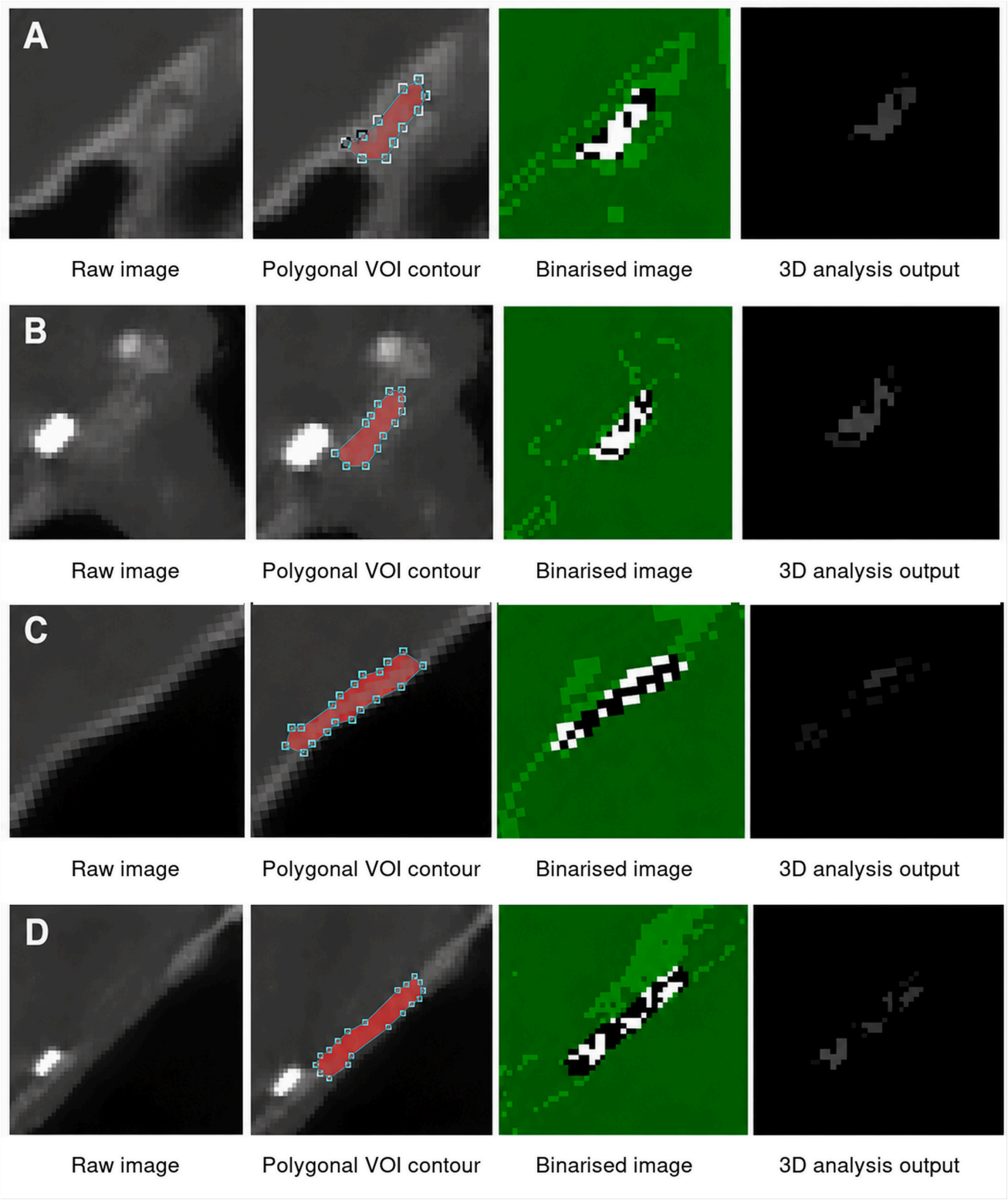


Figure 4

Representative image-processing workflow for three-dimensional fractal analysis. The rows show the preoperative piriform (A), postoperative piriform (B), preoperative zygomaticomaxillary (C) and postoperative zygomaticomaxillary (D) regions. From left to right, each row presents the raw axial image, freehand polygonal ROI delineation, binarised image obtained using the fixed threshold range and

segmented structure used for three-dimensional analysis. The polygonal ROIs delineated on consecutive axial slices collectively formed the corresponding VOI. ROI, region of interest; VOI, volume of interest